The Role of Bone Scanning in Osteomalacia

Ignac Fogelman, James H. McKillop, Rodney G. Bessent, Iain T. Boyle,
John G. Turner, and William R. Greig

The Royal Infirmary, Glasgow, Scotland

The presence of eight "metabolic features" was assessed on the bone scintigrams of ten patients with osteomalacia. In all of these bone images, sufficient features were present to strongly suggest a metabolic disorder. These scintiphotos were included in a controlled blind study using 30 normal bone scans and 20 scans of metastatic disease. Nine of the ten metabolic bone images were correctly identified by two independent observers. Skeletal uptake of radiotracer, expressed as bone-to-soft-tissue ratio, was significantly higher in the osteomalacic patients than in a group of 80 controls.

J Nucl Med 19: 245–248, 1978

Bone scanning is now established as a highly sensitive means of detecting bone metastases, and its superiority over radiographic detection is well recognized (*1,2*). Nevertheless, its use in metabolic bone disease has been limited, although several workers have suggested that it may have a useful role to play in these disorders (*3–7*). Using Tc-99m HEDP, we have obtained bone images in ten patients with osteomalacia, and this communication describes our findings.

METHODS

The study group consists of ten patients complaining of bone and muscle pain and with histologically proven osteomalacia from various causes (Table 1). In each patient multiple views of the skeleton were recorded on Polaroid film from a gamma camera fitted with a high-resolution medium-sensitivity collimator. Spinal views were obtained with 300,000 counts, and all other views with a minimum of 100,000 counts. Bone images were obtained 4 hr after the i.v. injection of 15 mCi of Tc-99m HEDP. The scintiphotos were evaluated for the presence of the following features, which although not necessarily specific have been reported in various metabolic bone diseases: (a) a subjective impression of increased tracer uptake by the axial skeleton (*4,8*), by the long bones (*3–5*), and by the wrists (*5*); (b) prominent calvarium and mandible (*3,7*); (c) beading of the costochondral junctions (*4,5*); and (d) faint kidney images (*4*). In addition, two other features—focal abnormalities representing pseudofractures (Fig. 1) (*9,10*) and a "tie" sternum (Fig. 2), which we have observed in osteomalacic patients —were also included. All of these "metabolic features" were scored either as absent, probably present, or definitely present. The ten sets of images were also included in a controlled blind study using 50 additional, randomly selected sets of bone scans: 30 normal studies and 20 showing metastatic disease. Two observers evaluated the 60 sets of bone images independently without knowledge of patient identification. Each image was recorded as normal, metastatic, or metabolic (Table 3).

In addition to the Polaroid prints, all images were recorded and stored on a minicomputer by means of an analog-to-digital interface. The pictures were stored on computer magnetic tape for later retrieval and processing, and were displayed on a color TV screen. Bone-to-soft-tissue ratios were measured by using the computer to define regions of interest around the L2 vertebra and an area just below the kidney on the TV image. In each area the ratio of the counts per unit area from the former region to the latter was calculated from the teletype printout of the total counts. Similarly, these ratios were calculated for a control group of 80 females with breast

Received July 26, 1977; revision accepted Oct. 18, 1977.
For reprints contact: I. Fogelman, Royal Infirmary, Dept. of Nuclear Medicine, Glasgow G4 OSF, Scotland.

TABLE 1. CLINICAL AND BIOCHEMICAL DATA FROM OSTEOMALACIC PATIENTS

Patient No., age, and sex	Diagnosis	Serum calcium (normal 2.2–2.6 mmol/l)	Serum phosphate (normal 0.8–1.4 mmol/l)	Serum alkaline phosphatase (normal 80–280 u/l)	Albumin (normal 35–55 g/l)
1. 34 M	Vitamin-D deficiency osteomalacia	1.8	1.5	1,501	38
2. 74 F	Vitamin-D deficiency osteomalacia	2.15	1.0	576	36
3. 68 F	Postgastrectomy osteomalacia	2.05	0.85	679	34
4. 23 F	Vitamin-D deficiency osteomalacia	2.0	1.3	990	33
5. 20 M	Crohn's disease osteomalacia	1.9	0.7	933	25
6. 30 F	Vitamin-D deficiency osteomalacia	2.1	0.75	1,195	40
7. 67 F	Postgastrectomy osteomalacia	1.8	1.2	1,004	41
8. 15 M	Vitamin-D deficiency osteomalacia	1.6	1.35	2,218	45
9. 33 M	Coeliac disease osteomalacia	1.9	0.8	1,391	45
10. 79 F	Anticonvulsant-induced osteomalacia	1.7	1.1	927	34

carcinoma (age range 32–84 yr) without either clinical or scintigraphic suspicion of bone metastases.

RESULTS

The relevant clinical and biochemical details of the osteomalacic patients are shown in Table 1.

Table 2 summarizes the qualitative and quantitative results of the scintigraphic studies in the osteomalacic patients. The mean bone-to-soft-tissue uptake ratio for the osteomalacic group was 6.57 $\pm$ 1.43 (s.d.), whereas that in the 80 control patients was 4.05 $\pm$ 0.69. Using the Wilcoxon rank sum test, the uptake in the osteomalacic group was significantly higher ($p < 0.001$).

The results of the controlled blind study of the 60 bone images are shown in Table 3. Both observers correctly identified all 30 normal studies and all 20 metastatic studies. Each observer also correctly identified nine of the ten images from the osteomalacic patients.

DISCUSSION

The bone-to-soft-tissue ratio is usually found to be normal in patients with primary hyperparathyroidism (*6,11*). Seven of our osteomalacic patients had elevated ratios compared to our control group; this suggests increased tracer uptake by the axial skeleton, but it was not always apparent from the Polaroid images (Table 2). An elevated bone-to-soft-tissue ratio, when present, however, will support a presumptive diagnosis of osteomalacia.

The most consistent subjective "abnormalities"

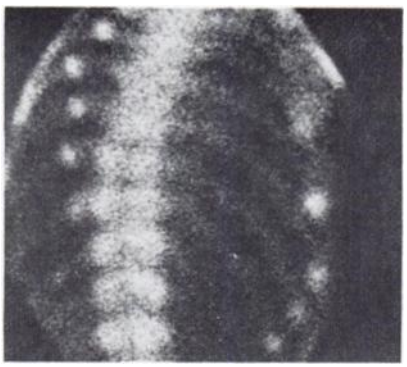

FIG. 1. Dorsolumbar spine. Multiple hot spots in ribs. Radiographs confirmed pseudofractures at these sites.

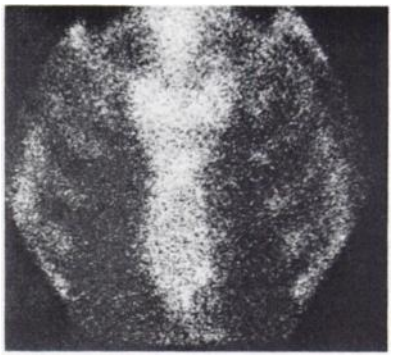

FIG. 2. Anterior view of chest with marked increased uptake of tracer by sternum, especially at its margins—so-called "tie sternum".

TABLE 2. BONE-TO-SOFT-TISSUE (B/ST) RATIOS AND SUBJECTIVE ASSESSMENT* OF SCAN IMAGES

Patient No.	Increased uptake of radiopharmaceutical by: Axial skeleton	Long bones	Wrists	Beading costochondral junction	"Tie sternum"	Hot spots (pseudofractures)	Prominent mandible and calvarium	Faint kidney images	B/ST ratio
1	+	+	++	++	++	++	++	+	4.7
2	+	++	++	+	++	++	++	++	7.8
3	+	++	++	−	−	++	+	++	5.0
4	++	++	not recorded	++	++	++	++	++	7.6
5	++	++	++	+	−	++	++	+	6.9
6	++	++	++	+	−	++	++	++	9.0
7	++	+	++	+	++	++	−	+	4.9
8	++	++	++	++	+	−	++	++	7.2
9	+	++	++	++	+	++	++	+	6.8
10	+	++	+	−	+	++	+	+	5.8

* Absent —; Probably present +; Definitely present ++.

TABLE 3. CONTROLLED BLIND ASSESSMENT OF BONE SCINTIGRAMS

	Metabolic	Metastatic	Normal
Number	10	20	30
Observer J.G.T.	9	21	30
Observer J.H.McK.	9	21	30

noted on the bone images were increased uptake of radiopharmaceutical by the long bones and wrists, with apparent prominence of the calvarium and mandible (Table 2). However, these appearances are nonspecific and are found in other metabolic conditions such as hyperparathyroidism (*4*). Other useful indications of a metabolic disorder—although seen less often in our cases—were the presence of beading of the costochondral junctions, and the "tie sternum." Again, these features may be nonspecific in that they can be seen in patients with renal osteodystrophy, although there is often a significant degree of osteomalacia in such patients.

Although the kidneys were visualized in all patients, in five the kidneys were faint, perhaps reflecting reduced excretion of tracer by the kidneys due to increased skeletal uptake. Pseudofractures were detected in nine patients. In one patient, the previous radiological skeletal survey had been normal, whereas on the scintigram multiple hot spots were seen over the ribs. Subsequent coned radiographs of the areas of abnormality confirmed the presence of several pseudofractures, although these were still not seen in some of the areas indicated by the bone study. In the other patients, routine radiographs identified pseudofractures at the sites of abnormality seen on the bone image. In two patients, however, pelvic pseudofractures shown unequivocally by conventional radiology were not detected on initial scan interpretation. On review of the bone images it was apparent that in one patient there were scintigraphic abnormalities attributable to the pseudofractures, but these had been missed because of their symmetrical nature. In the second patient, no pelvic abnormality was detectable, even on review.

Although the bone images in osteomalacia appear to be nonspecific, we considered that in all our patients, the scintigrams strongly suggested a metabolic disorder. These images were therefore included in a controlled blind study with 50 sets of normal and metastatic bone scintigrams. Table 3 shows that nine of the ten sets of metabolic scans were diagnosed as such by two independent observers. There was complete agreement on all the normal and metastatic images, and on eight of the metabolic ones. No normal or metastatic scan was recorded as metabolic. Each observer considered one osteomalacic scan to be metastatic, and these scans had multiple focal abnormalities representing pseudofractures. Thus an awareness of "metabolic features" on a bone image may alert one to the presence of a metabolic disorder, often with high probability. However, the bone-scan appearances are nonspecific and it is important that adequate clinical information be available during the reading of such scans, since the presence of focal abnormalities, for example, can be mistaken for other conditions, such as metastatic disease.

The bone scintigram, therefore, has a role to play in the detection of osteomalacia, since a combination of several "metabolic features," together with a raised bone-to-soft-tissue ratio, support this diag-

nosis. Multiple focal defects in such an image suggest the presence of pseudofractures, although other conditions cannot be excluded. Roentgenographs of such lesions are mandatory.

REFERENCES

1. CHARKES MD: Bone scanning: Principles, technique and interpretation. *Radiol Clin N Am* 8: 259–270, 1970

2. VERDON TA, YANO Y, ANGER HO: The use of radionuclides in the detection of bone metastases. *J Surg Oncol* 3: 665–672, 1975

3. SY MW: Bone scan in primary hyperparathyroidism. *J Nucl Med* 15: 1089–1091, 1974

4. SY WM, MITTAL AK: Bone scan in chronic dialysis patients with evidence of secondary hyperparathyroidism and renal osteodystrophy. *Br J Radiol* 48: 878–884, 1975

5. ROSENTHALL L, KAYE M: Technetium-99m-pyrophosphate kinetics and imaging in metabolic bone disease. *J Nucl Med* 16: 33–39, 1975

6. WIEGMANN T, ROSENTHALL L, KAYE M: Technetium-99m-pyrophosphate bone scans in hyperparathyroidism. *J Nucl Med* 18: 231–235, 1977

7. KRISHNAMURTHY GT, BRICKMAN AS, BLAHD WH: Technetium-99m-Sn-pyrophosphate pharmacokinetics and bone image changes in parathyroid disease. *J Nucl Med* 18: 236–242, 1977

8. FOGELMAN I, MCKILLOP JH, BOYLE IT, et al: Absent kidney sign associated with symmetrical and uniformly increased uptake of radiopharmaceutical by the skeleton. *Eur J Nucl Med*: in press

9. SINGH BN, KESALA BA, MEHTA SP, et al: Osteomalacia on bone scan simulating skeletal metastases. *Clin Nucl Med* 2: 181–183, 1977

10. FOGELMAN I, MCKILLOP JH, GREIG WR, et al: Pseudofractures of the ribs detected by bone scanning. *J Nucl Med* 18: 1236, 1977

11. FOGELMAN I, BESSENT RG, BOYLE IT, et al: Skeletal uptake of Tc-99m HEDP in primary hyperparathyroidism. *J Nucl Med* 18: 1040, 1977